Article

Nano-Additives in Asphalt Binder: Bridging the Gap between Traditional Materials and Modern Requirements

Amjad H. Albayati [1] , Roaa H. Latief [1], Hasan Al-Mosawe [2,*] and Yu Wang [3]

1 Department of Civil Engineering, College of Engineering, University of Baghdad, Baghdad 10071, Iraq; a.khalil@uobaghdad.edu.iq (A.H.A.); roaa.hamed@coeng.uobaghdad.edu.iq (R.H.L.)
2 Civil Engineering Department, College of Engineering, Al-Nahrain University, Baghdad 10071, Iraq
3 School of Science, Engineering and Environment, University of Salford, Manchester M5 4WT, UK; y.wang@salford.ac.uk
* Correspondence: hasan.m.al-mosawe@nahrainuniv.edu.iq

Abstract: This research delves into the realm of asphalt technology, exploring the potential of nano-additives to enhance traditional asphalt binder properties. Focusing on Nano-Titanium Dioxide (NT), Nano-Aluminum Oxide (NA), and Nano-Silica Oxide (NS), this study investigates the effects of incorporating these nanomaterials at varying dosages, ranging from 0% to 8%, on the asphalt binder's performance. This study employs a series of experimental tests, including consistency, storage stability, rotational viscosity, mass loss due to aging, and rheological properties, to assess the impact of nano-additives on asphalt binder characteristics. The findings indicate a substantial improvement in the consistency of the asphalt binder with the addition of nanomaterials, particularly NS, which shows a 41% reduction in penetration at an 8% content and a notable increase in the softening point. The storage stability tests reveal that NS-modified asphalt exhibits superior stability compared to NT and NA, with a significantly lower ΔT increase. Furthermore, the investigation into rotational viscosity suggests that NS, despite increasing the binder's viscosity, does not exceed the AASHTO M320 threshold, ensuring the binder's workability. Aging tests demonstrate that NT, at lower concentrations, acts as an effective anti-aging agent, whereas NA and NS tend to increase the mass loss, impacting thermal stability. This study concludes that while each nanomaterial uniquely influences the asphalt binder's properties, NS stands out in terms of enhancing the high-temperature performance and storage stability. Optimal dosages of 6% for NT and NA and 4% for NS are recommended based on the Overall Desirability analysis. This research bridges the gap between traditional asphalt materials and modern requirements, highlighting the transformative impact of nano-additives in advancing asphalt pavement technology.

Keywords: Nano-Titanium Dioxide; Nano-Aluminum Oxide; Nano-Silica Oxide; asphalt binder rheology; asphalt binder consistency

1. Introduction

The most common type of pavement, flexible pavement, is favored for its acceptable performance under repeated loads and various environmental conditions. Recently, however, this type of pavement has faced challenges due to increased traffic loads and extreme climate conditions. Consequently, this exposure often leads to significant damage in the early stages of the pavement's life, as evidenced by the prevalence of fatigue cracks, moisture damage, permanent deformations, and other defects. Such deterioration can adversely impact the comfort and safety of road users. Consequently, the maintenance and repair of such pavement failures become costly [1]. In an effort to prevent failures and achieve more cost-effective pavements, numerous methods have been developed to enhance the performance and extend the service life of flexible pavements [2–6]. One of the most effective methods is the modification of asphalt with various additive materials to

improve the virgin asphalt cement's performance characteristics. These additives include polymers, fibers, and nanomaterial (NM), each contributing to enhancing the binder and asphalt concrete properties [7–16].

Nanotechnology has experienced rapid development across various fields. In the realm of asphalt pavement, the addition of NMs to enhance the properties of asphalt binders has gained popularity over the past decade. This trend developed due to the unique attributes of NMs, such as their high stability, large surface area, chemical purity, and effective dispersion ability. Notably, there are significant differences in the chemical and physical properties of original raw materials and their nanoscale counterparts [17].

Basically, NMs are produced by reducing the dimensions of materials from a normal or original size to nano size, resulting in noticeable changes in the characteristics of the original materials, such as their mechanical properties and chemical reactivity. These materials typically have at least one dimension within the range of 1 to 100 nanometers and exhibit an increased surface area due to a higher proportion of atoms on the surface. This size reduction leads to altered surface morphologies, surface energies, and physicochemical properties of the original material [18–23].

Research over the past decade, as summarized in Table 1, has focused on individual nanomaterial modifications in asphalt binders. This study expands upon these works by investigating three nanomaterials, NT, NA, and NS, at dosages of 0%, 2%, 4%, 6%, and 8% by weight of asphalt cement. Utilizing an Overall Desirability (OD) analysis, this research evaluates multiple properties such as penetration, softening point, and viscosity, aiming to determine optimal nanomaterial dosages for improved pavement performance. This comprehensive approach not only bridges the gaps of previous studies but also establishes guidelines for effective nanomaterial use for asphalt binder modifications.

Table 1. Summary of research works using NT, NA, and NS to modify asphalt binder.

Ref.	Year	Binder Type	Type of NM	NM Dosage (% by Weight of Asphalt)	Main Conclusions
US [24]	2011	PG 64-16	NT	0, 3, 5, 7	NT did not affect physical properties of virgin binder
Malaysia [19]	2014	Polymer-modified asphalt (PG-76)	NS	0, 2, 4	Scanning electron microscopy (SEM) analysis revealed that NS particles were scattered uniformly throughout asphalt binder, which is better than polymer dispersion
China [25]	2015	AC 70	NT	0, 2	-Highly effective in improving Ultraviolet (UV) aging resistance through NT surface modification -Enhanced compatibility between asphalt binder and NT by using surface modification
Saudi Arabia [26]	2016	AC (60-70)	NA	0, 3, 5, 7	-NA modification increased asphalt thickness because of rise in viscosity of asphalt binder, which presented better coating of aggregate particles in asphalt mixture -At high temperatures, asphalt binders have great storage stability at 5% NA modification because agglomeration will occur and increase through asphalt binder at 7% NA, which means it is less stable -5% NA sample has highest rutting parameter (G*/sin δ)

Table 1. *Cont.*

Ref.	Year	Binder Type	Type of NM	NM Dosage (% by Weight of Asphalt)	Main Conclusions
Turkey [27]	2017	PG 64-22	NS	0, 0.1, 0.3, 0.5	-Enhanced anti-cracking performance and rutting resistance for asphalt binder with addition of 0.3% of NS -NS modification improved energy savings
Iran [28]	2017	AC (60-70)	NA	0, 0.3, 0.6, 0.9, 1.2	-Permanent deformation and final strain were decreased for NA-modified stone mastic asphalt -Addition of NS increased viscosity and softening point (SP) of asphalt binder
Egypt [29]	2017	AC (60-70)	NS	0, 2, 4, 6	-No negative effect on temperature susceptibility (TS) for NS-modified asphalt binder -Penetration grade decreased in NS-modified binder compared to base asphalt -Increased viscosity of binder with increased addition of NS
China [30]	2018	AC (60-70)	NS	0, 0.1, 0.2, 0.3	-Increasing NS dosage improves complex modulus of asphalt binder -SEM image analysis revealed that NS activity would decline because agglomerations throughout asphalt matrix caused reduction in bonding force between NS particles and decrease in specific surface area
China [31]	2019	SBS-modified asphalt	NT	0, 1, 2, 5, 10	-Highly effective in improving rutting resistance and aging performance of SBS-modified asphalt with addition of 1% NT -At low temperature, NT had no positive influence on cracking resistance of SBS-modified asphalt because creep rate and creep stiffness are almost identical for all samples
Malaysia [32]	2019	AC (80/100)	NT	0, 2, 4, 6, 8, 10	-Penetration grade is decreased, accompanied by slight increase in SP, which clearly indicates effect of NT on stiffness of modified asphalt binder -As seen in SEM images, NS particles disperse successfully and homogeneously throughout asphalt binder structure
Iran [33]	2019	AC (60-70)	NS	0, 2, 4, 6	-Stiffness and cohesion are decreased for NS-modified binder compared to base asphalt -Decreased TS for binder with addition of NS

Table 1. *Cont.*

Ref.	Year	Binder Type	Type of NM	NM Dosage (% by Weight of Asphalt)	Main Conclusions
Turkey [34]	2020	AC (50/70)	NT	0, 2, 4	-Penetration grade is decreased, accompanied by slight increase in SP, clearly indicating effect of NT on stiffness of modified binder -Higher Penetration Index signifies that NT has positive influence on TS of asphalt binder -Loss of weight of NT-modified asphalt binder decreases slightly after short-term aging process -After NT modification, there is no progress in terms of high temperature for performance grade
Turkey [35]	2020	AC (50/70)	NA	0, 3, 5, 7	-5% NA achieved best anti-rutting performance and fatigue cracking of modified asphalt binder due to increase in value of $G^*/\sin\delta$ and decrease in value of $G^*\sin\delta$, respectively -SEM analysis revealed that some NA particles fully dispersed and other NA particles caused little agglomeration throughout asphalt binder -Based on rotational viscometer test results, mixing and compaction temperatures decreased for NA-modified asphalt binder, which was considered economic advantage -No change in performance grades for NA-modified binder compared to reference binder
India [36]	2020	AC—viscosity grade 10 (VG-10)	NA	0, 0.5, 1, 2	-NA particles have crystalline nature compared to base asphalt because XRD analysis showed that NA has distinct peaks -2% NA achieved best anti-rutting performance of modified asphalt binder due to increase in the value of Superpave rutting parameter, $G^*/\sin\delta$ -Complex modulus increased, and phase angle decreased for NA-modified asphalt binder; this confirmed that adding NA makes binder elastic and stiffer in nature
India [37]	2021	SBS-modified asphalt	NA	0, 1, 2, 3, 4, 5	-Fatigue life and anti-rutting behavior of NA-SBS-modified binder are improved -After adding NA, storage stability and aging resistance of asphalt binder are significantly enhanced
Malaysia [38]	2022	AC (60-70)	NT	0, 1, 2, 3, 4, 5	-NT modification improved mechanical and volumetric properties of stone mastic asphalt -Excellent enhancement in terms of chemical and morphological properties with 3% NT addition

Table 1. *Cont.*

Ref.	Year	Binder Type	Type of NM	NM Dosage (% by Weight of Asphalt)	Main Conclusions
Turkey [39]	2022	AC (60-70)	NA	0, 3, 5, 7	-Penetration grade decreased, accompanied by increase in SP, clearly indicating that NA affects stiffness of modified asphalt binder -Binder viscosity is increased after NA modification -At high temperature, NA-modified asphalt binder has less sensitivity to permanent deformation due to reduction in creep compliance parameter
Iraq [40]	2023	AC (40-50)	NS	0, 2, 4, 6	Microstructural analysis revealed that NS particles disperse homogeneously throughout asphalt binder structure due to good dispersion potential and large specific surface area of NS
Current Study	2024	AC (40-50)	NT NA NS	0, 2, 4, 6, 8	Current study aims to evaluate the following: -Crystalline structure of each NMs using SEM; -Change in asphalt binder consistency of virgin and modified asphalt cements; -Change in storage stability of different modified binders; -Mass loss due to short-term aging of virgin and modified asphalt cements; -Workability of asphalt cement (virgin and modified) by implementing rotational viscosity test at different temperatures (for original and aged asphalt); -Rheological properties of virgin and modified asphalt cements, including rutting and fatigue index by using Dynamic Shear Rheometer (DSR).

2. Materials

2.1. Asphalt Cement

The base binder for this study is a 40/50 penetration grade asphalt cement, procured from the Dora refinery in Baghdad's southwest, which was chosen for its compliance with regional pavement standards. Its physical properties, listed in Table 2, align with the stringent requirements for conventional pavement materials. Table 3 details the binder's rheological properties, affirming its classification under the Performance Grade (PG) 64-16, as stipulated by [41]. This grade ensures the asphalt cement's resistance to temperature-induced rutting and cracking, providing an ideal foundation for assessing the impact of nano-additives on asphalt property enhancements.

Table 2. The test results for the physical properties of asphalt cement.

Property	Standard	Test Result	Specification Limit
Penetration at 25 °C, 100 gm, 5 s. (0.1 mm)	[42]	49	(40–50)
Ductility at 25 °C, 5 cm/min. (cm)	[43]	110	>100
Flashpoint (Cleveland open cup) (°C)	[44]	311	Min. 232
Softening point (°C)	[45]	49.7	-
Specific gravity at 25 °C	[46]	1.04	-
The residue from thin film oven test	[47]	-	
Retained penetration (% of original)	[48]	58	
Ductility at 25 °C, 5 cm/min (cm)	[49]	80	-

Table 3. Rheological properties of asphalt cement.

Asphalt Cement	Properties	Temperature Measured °C	Measured Parameters	Specification Requirements, [41]
Original	Flash point (°C)	-	311	230 °C, min
	Viscosity at 135 °C (Pa·s)	-	719.7	3000 m Pa·s, max
	DSR, G/sinδ at 10 rad/s (kPa)	58	3.4515	
		64	1.6623	1.00 kPa, min
		70	0.8425	
RTFO Aged	Mass loss (%)	-	0.266	1%, max
	DSR, G/sinδ at 10 rad/s (kPa)	58	6.8651	
		64	3.4578	2.2 kPa, min
		70	1.7241	
PAV Aged	DSR, G.sinδ at 10 rad/s (kPa)	28	3485	5000 kPa, max
		25	5068	
	BBR, creep stiffness (MPa)	−6	183	300 MPa, max
	Slope m-value	−6	0.368	0.3, min

2.2. Nanomaterials

The nanomaterials NT, NA, and NS exhibit distinct physical properties, making them invaluable in enhancing the performance of asphalt mixtures. NT is noted for its high purity and substantial specific surface area, NA is noted for its remarkable melting point, and NS is noted for its exceptional specific surface area and particle size range. The major physical properties of these nanomaterials are meticulously detailed in Table 4, providing a foundation for their selection and utilization in this research. A photograph showing these nanomaterials is presented in Figure 1.

Table 4. Physical properties of nanomaterials.

Properties	Nanomaterial		
	NT	NA	NS
Chemical formula	TiO_2	Al_2O_3	SiO_2
Molecule wt. (g/mol)	85.42	101.96	60.08
Appearance	White Powder	White Powder	White Powder
Average particle size (nm)	20–30	10–20	25–35
Purity (%)	99.9	99.9	99.8
Specific surface area (m^2/gm)	120–160	120–160	190–250
Meting point (°C)	1860	2030	1730
Bulk Density (g/mL)	0.51	0.2	0.08
Ph	5.5–6.5	8.5–9.5	5–6.5

Figure 1. Photograph of nanomaterials.

Scanning Electron Microscope (SEM) images at 120,000× magnification, as exhibited in Figure 2, provide a detailed portrayal of the nanostructured materials examined in this research. The SEM image of NT indicates a predominant cluster form of spherical particles, which has a fairly even size due to van der Waals forces or interfacial surface charge interactions. The uniformity and spherical nature of the particles suggest that NT could provide a consistent surface area to facilitate the mix with the asphalt binder, potentially leading to uniform dispersion within the mixture. The particle size, within the tens of nanometers range, aligns with the enhanced properties that are typically sought in nanomaterials, such as increased reactivity and strength when applied in a binder matrix.

In contrast, the SEM image of NA features a diverse range of agglomerated particles with a more irregular morphology than the aforementioned NT. The agglomerates are less uniform in shape, displaying a varied structure that could suggest more complex surface interactions with the asphalt binder. This irregularity might influence both interlocking and dispersion within the asphalt, potentially affecting the mechanical reinforcement that NA provides.

The SEM image of NS displays a highly dense and somewhat homogenous cluster of particles, with a textured surface indicative of a high surface area. The particles exhibit an amorphous structure with less defined shapes compared to NT and NA. This morphology indicates that NS particles may provide a substantial contact area for interaction with the asphalt binder, which could increase the binder's stiffness, thereby significantly reducing its fluidity. Consequently, this prevents the aggregate particles from easily sliding among each other. This resistance to particle movement is crucial for reducing the likelihood of permanent deformation under the high temperatures typically encountered during the pavement service life.

This morphological analysis lays critical groundwork for understanding how these nanomaterials may physically and chemically integrate with the asphalt binder.
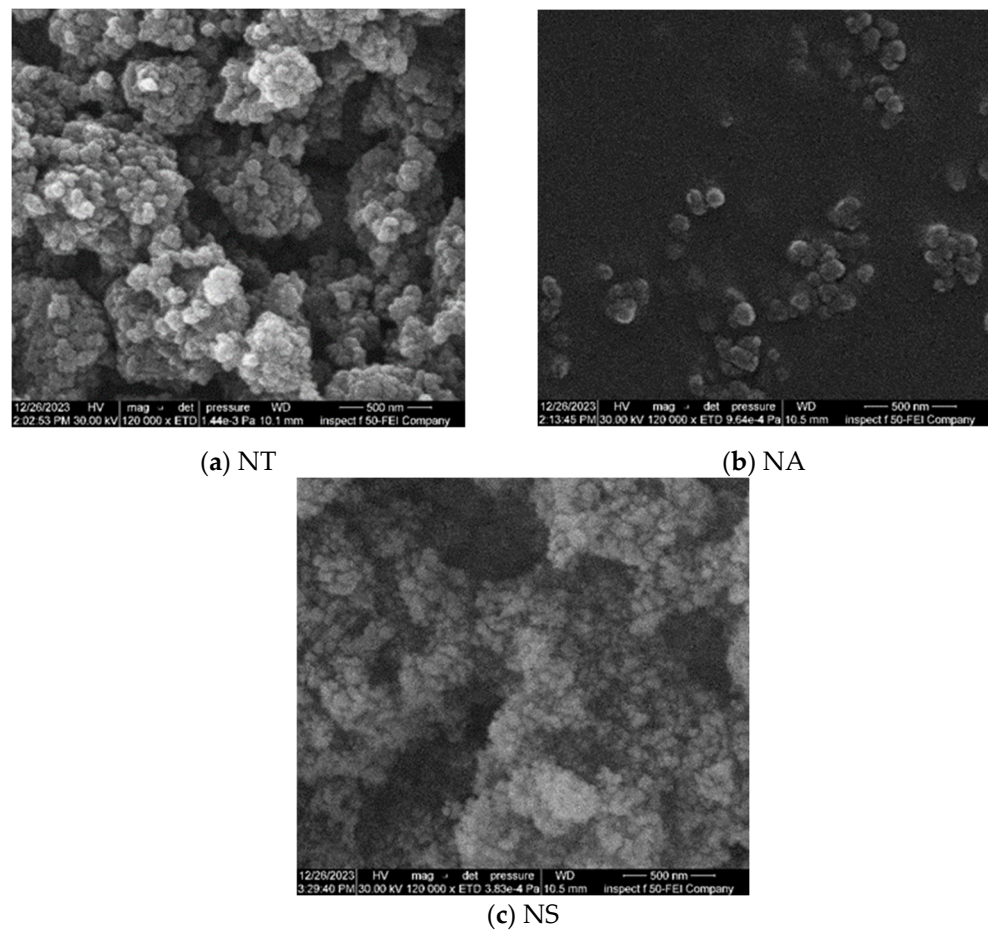
(**a**) NT   (**b**) NA

(**c**) NS

Figure 2. SEM images of nanomaterials.

2.3. Nanomaterial Addition Method

In this research, a high-speed stirring technique was employed to uniformly distribute NT, NA, or NS within Performance Grade (PG) 64-16 asphalt cement. These nanomaterials were introduced at concentrations of 2, 4, 6, and 8% by weight of the asphalt cement alongside a baseline sample of unmodified asphalt. The incorporation process utilized a high-speed shear mixer system (HSMS), which is notably different from traditional mixers in terms of its operational mechanism.

The procedure began with heating the neat asphalt cement, weighing approximately 400 g, to 140 °C. This was followed by 20 min of mechanical mixing. Subsequently, the nanomaterials were incrementally introduced to the heated binder at a consistent rate of 4 g per minute, with the mixing sustained at 4000 rpm. This meticulous addition and mixing protocol was crucial for ensuring the nanoparticles were evenly distributed throughout the binder. Designed to create a homogeneous mixture and to prevent premature aging of the bitumen, this method was rigorously adhered to. After completing the mixing process, the nano-modified asphalt was transferred to metal containers to cool at room temperature, preparing it for further analysis.

3. Experimental Tests

A series of experimental tests were conducted to evaluate the consistency, storage stability, rotational viscosity, mass loss due to aging, and rheological properties to assess the impact of nano-additives on asphalt binder characteristics. Sample preparation and testing procedures were meticulously followed according to the specified ASTM standards for each test, which are listed below.

3.1. Consistency Properties

The initial phase of binder testing focused on evaluating the basic physical properties that are essential for determining the consistency and performance of asphalt binders. This phase included conducting the penetration test [42], which measures the depth that a standard needle penetrates the asphalt binder under specific conditions, offering insights into the binder's consistency. Simultaneously, the softening point (SP) test was carried out according to [45] to determine the temperature at which the asphalt binder transitions from a semi-solid state to a liquid state, providing a critical measure of the binder's susceptibility to high temperatures. Additionally, the Penetration Index (PI) was calculated to quantify the asphalt binder's sensitivity to temperature variations. This index, derived from the results of the softening point and penetration at 25 °C, is calculated using the following formula:

$$\text{PI} = \frac{1952 - 500\log P25 - 20SP}{50\log P25 - SP - 120} \tag{1}$$

where P25 denotes the penetration value at 25 °C, and SP signifies the softening point. These tests collectively form the cornerstone of binder assessment, establishing a foundational understanding of the asphalt binder's physical characteristics and its expected performance in various environmental conditions.

3.2. Storage Stability

The storage stability test, which is crucial for evaluating the uniform dispersion of nanomaterial modifiers such as NT, NA, and NS, follows the [46] guidelines. This assessment aims to identify any potential sedimentation of nanomaterials within an asphalt binder during storage by measuring the difference in softening points (ΔT) between the top and bottom samples extracted from the test tube. This measurement indicates the presence of any separation or settling of nanomaterials within the binder. The conditioning procedure includes placing samples into cylindrical molds measuring 32 mm in diameter and 160 mm in height, which are then heated in an oven at 163 °C for 72 h before being allowed to cool at room temperature. The effectiveness of the mixing conditions was confirmed, as evidenced by the ΔT values, which remained below the acceptable limit of 2.2 °C, thus indicating that the nanomaterials were evenly distributed without significant separation.

3.3. Mass Loss

In this experimental work, the Rolling Thin Film Oven (RTFO) test was conducted as per the [47] requirement to quantify the mass loss in asphalt binders, including those modified with nanomaterials. This test is vital as it simulates short-term aging by heating the samples at 163 °C (325 °F) for 85 min, thereby assessing the binder's thermal stability. The primary objective was to determine the mass loss upon heating, providing crucial insights into the volatile content of the binder. This aspect is significant for understanding and predicting the long-term performance and durability of both traditional and nanomaterial-modified asphalt binders.

3.4. Rotational Viscosity

The rotational viscosity test, as outlined in [48], plays a pivotal role in determining the viscosity of asphalt binders at key temperatures of 115, 135, and 155 °C. This assessment is critical for understanding the binder's flow characteristics, directly impacting its ease of mixing and compaction during asphalt production. By measuring how the binder behaves at these specific temperatures, the test provides invaluable insights into the workability of the asphalt mixture. High temperatures typically reduce viscosity, facilitating easier mixing with aggregates and compaction into a dense, uniform pavement structure. Consequently, this test is instrumental in ensuring that asphalt binders meet the necessary standards for efficient application and optimal pavement performance.

3.5. Dynamic Shear Rheometer

The Dynamic Shear Rheometer (DSR) test, as outlined in [49], was pivotal in investigating the viscoelastic characteristics of both the original asphalt and nano-modified asphalt, playing a key role in determining their high-temperature performance and deformation resistance. Critical benchmarks for preventing long-term deformation were established, with a G*/sin δ threshold of over 1 kPa for original bitumen and 2.2 kPa for RTFO-aged asphalt. Additionally, the Pressure Aging Vessel (PAV) test was utilized to reduce the risk of long-term fatigue cracking, setting a maximum G*.sin δ of less than 5 kPa for aged bitumen at specific testing temperatures. These evaluations provide a comprehensive understanding of the asphalt binder's capabilities, highlighting its workability, durability against aging, and stability under varying temperatures, thereby contributing to the creation of superior-quality asphalt mixtures.

4. Results and Discussion

4.1. Consistency Test Results

The addition of nanomaterials notably affects the consistency properties of asphalt binders, as evidenced in Figures 3 and 4. The penetration values decrease consistently with the addition of nanomaterials; an 8% NT content correlates with an approximate 18% reduction in penetration relative to the neat asphalt cement, while NA and NS lead to 26% and 41% reductions, respectively. The significant impact of NS may be attributed to its high specific surface area, ranging from 190 to 250 m^2/g. Also, the SEM images reveal that the densely clustered particles of SiO_2 offer a substantial interface for interactions with the asphalt binder, significantly enhancing the binder's stiffness.
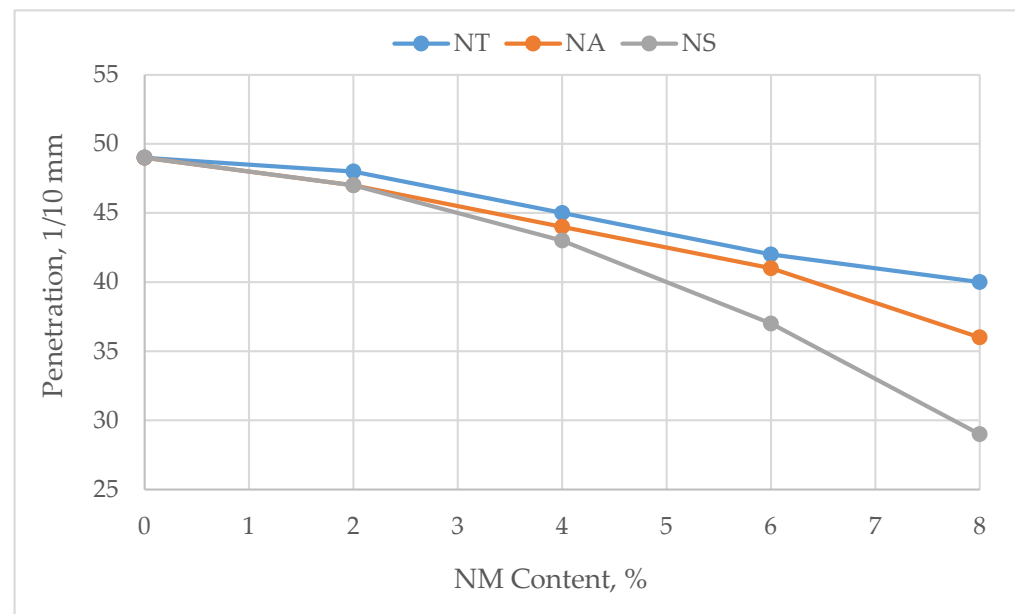

Figure 3. Effect of nanomaterials on penetration values.

In contrast, the softening points, as illustrated in Figure 4, exhibit an increase, suggesting improved resistance to high temperatures. The softening point for NT rises by approximately 6.8%, that for NA rises by 9.8%, and that for NS rises by an impressive 12.1% at the highest nanomaterial content compared to the neat asphalt cement.

These trends are corroborated by the Penetration Index (PI) values listed in Table 5, where the PI decreases as the nanomaterial content increases. This decrease in the PI indicates a higher stiffness and reduced temperature susceptibility for the nano-modified binders, marking a considerable enhancement in their thermal and mechanical performance. The softening point increase and penetration decrease collectively suggest a considerable

improvement in the asphalt binder's ability to maintain structural integrity under varying temperature conditions, solidifying the nanomaterials' role in the evolution of asphalt pavement engineering.
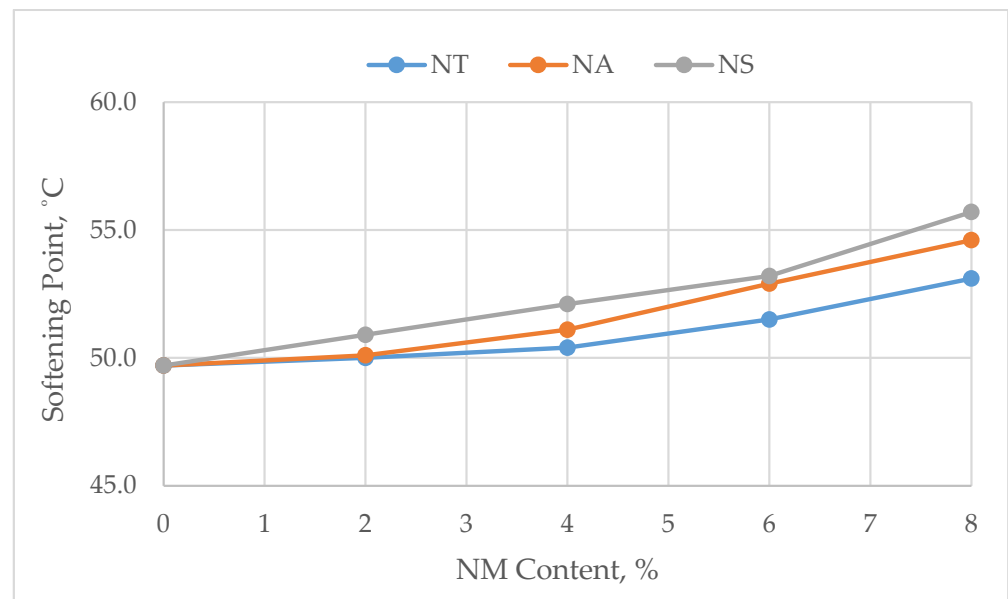

Figure 4. Effect of nanomaterials on softening point.

Table 5. Effect of nanomaterials on PI.

Nanomaterial	0%	2%	4%	6%	8%
NT	−1.33	−1.30	−1.34	−1.22	−0.96
NA	−1.33	−1.32	−1.22	−0.95	−0.85
NS	−1.33	−1.12	−1.03	−1.10	−1.04

4.2. Storage Stability Results

Figure 5 presents the results of the storage stability tests, illustrating how asphalt binders modified with nanomaterials retain compatibility. An upward trend in the ΔT values is observed with increasing nanomaterial concentrations. The NS-modified asphalt binder exhibits more favorable storage stability than those modified with NT and NA, as indicated by its consistently lower ΔT measurements. As the nanomaterial content increases, NS-modified binders show enhanced storage stability compared to NT and NA modifications. For example, the ΔT for NS-modified asphalt with an 8% inclusion is 1.3 °C, representing a 225% increase over the neat asphalt baseline of 0.4 °C, yet it remains within the compatibility threshold. By contrast, the NT- and NA-modified binders show ΔT increases of 400% and 300%, respectively, at the same inclusion rate. This enhanced storage stability of NS can be attributed to its lower density of 0.08 g/mL, compared to 0.51 g/mL for NT and 0.2 g/mL for NA, as detailed in Table 4, which promotes a more even distribution within the asphalt and reduces the potential for particle settling.

Despite the higher densities of materials like NT and NA, all modified binders keep ΔT values within the acceptable range for compatibility with the asphalt binder, set below 2.2 °C. This assures that, notwithstanding the different densities of the nanomaterials, the modified binders maintain the homogeneity necessary for practical application. The results suggest that the careful selection and quantification of nanomaterials can effectively enrich the asphalt binder's performance while ensuring its stability during storage.
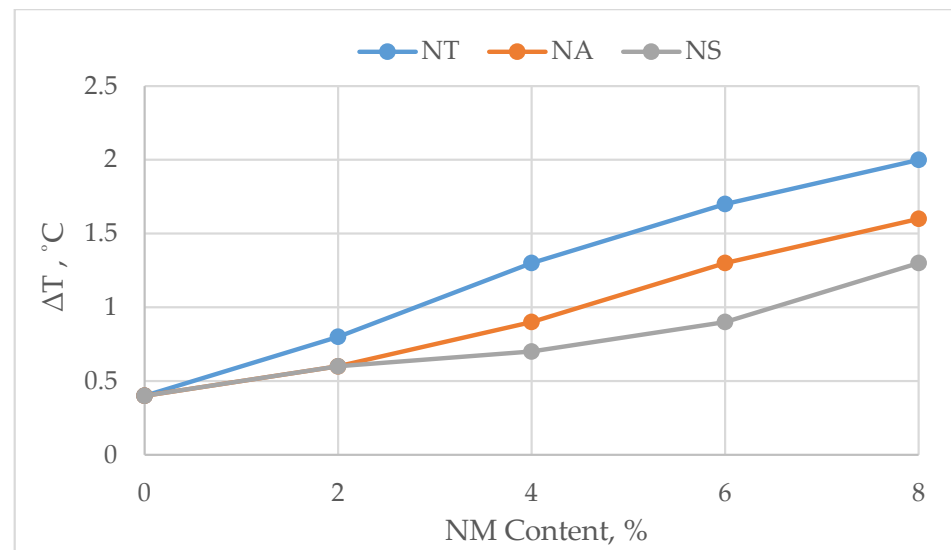
Figure 5. Effect of nanomaterials on storage stability.

4.3. Rotational Viscosity Results

The data presented in Figures 6 and 7 highlight the workability of asphalt binders, both in their original form and after undergoing the Rolling Thin Film Oven (RTFO) test. These figures reveal the effects of nanomaterials—NT, NA, and NS—on binder viscosity at varying temperatures: 115 °C, 135 °C, and 155 °C. Initially, a clear increase in viscosity with the addition of nanomaterials is observed, as shown in Figure 6. At 115 °C, viscosity starts at 2268 mPa·s for the neat binder and increases with the nanomaterial content, notably peaking at 5416.7 mPa·s for NS at an 8% dosage.
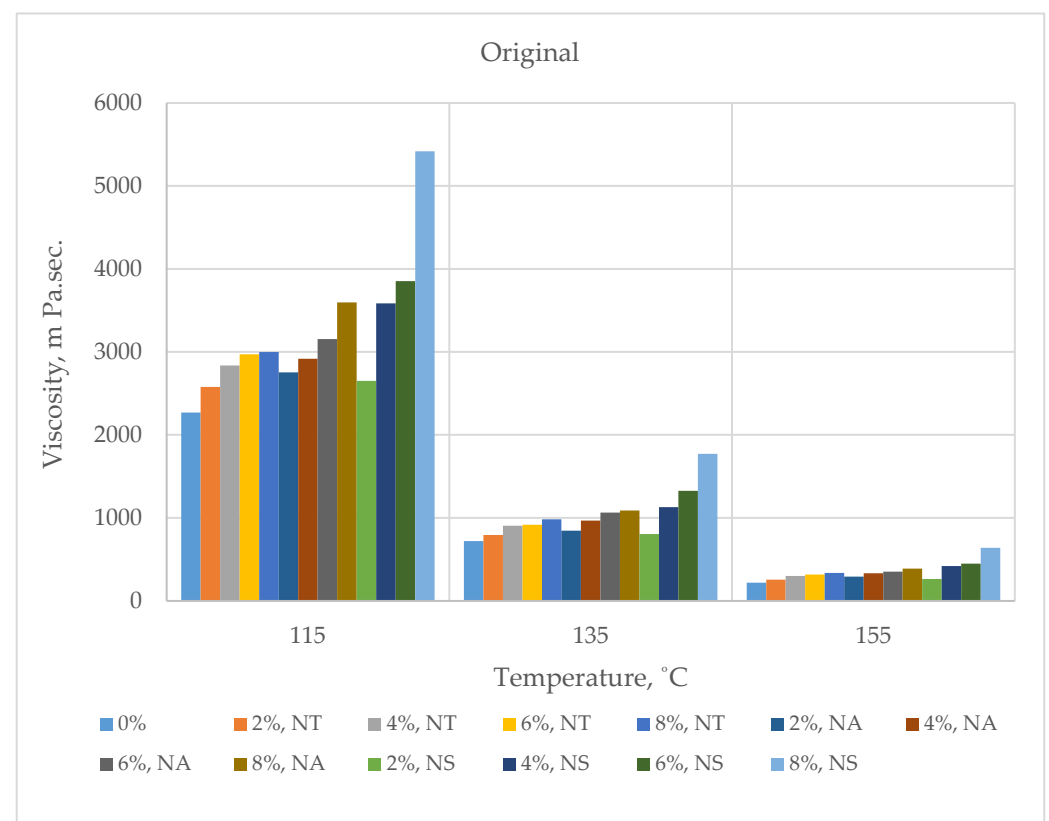

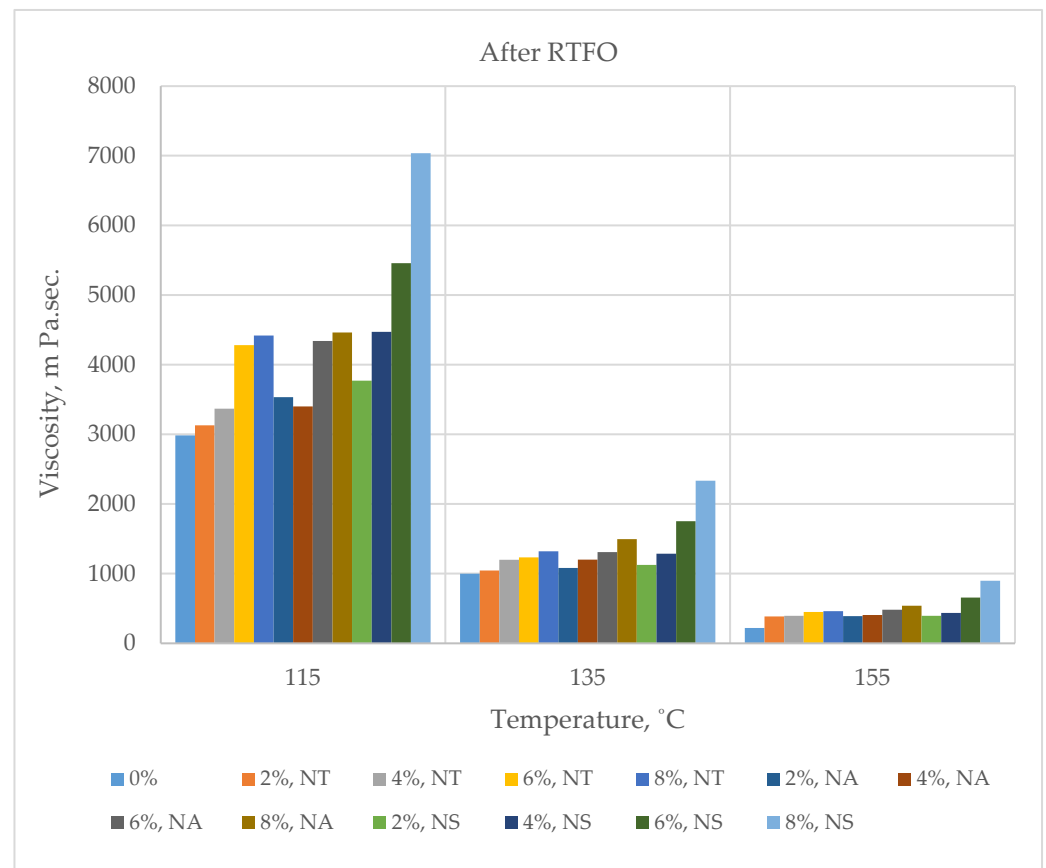**Figure 6.** Effect of nanomaterials on original binder RV.

Figure 7. Effect of nanomaterials on aged binder RV.

After RTFO aging, as indicated in Figure 7, there is an overall increase in viscosity, reflecting the stiffening effect of thermal exposure. Yet, even at the highest nanomaterial content, the viscosities remain below the threshold of 3000 mPa·s at 135 °C set by [41], ensuring the binders' suitability for paving operations. A review of the average viscosities across all dosages, detailed in Table 6, shows significant differences among the nanomaterial-modified binders. At 135 °C, NS records the highest average viscosity at 1150.1 mPa·s, a notable increment of about 33% compared to the neat binder's average of 863.3 mPa·s. In contrast, NT and NA exhibit lower average viscosities of 863.3 mPa·s and 936.56 mPa·s, representing increases of 16.6% and 8.5%, respectively. This suggests that NS's distinct morphology and high surface area significantly contribute to the viscosity increase. Furthermore, the chemical interactions between the NMs and asphalt components alongside the homogeneous distribution of nanoparticles, as evidenced in their storage stability, also play essential roles in these viscosity changes.

Table 6. Effect of nanomaterials on average RV values.

| | RV Values (mPa·S) | | | | | |
| Temperature | NT | | NA | | NS | |
	Original	After TFOT	Original	After TFOT	Original	After TFOT
115 °C	2730.12	3634.92	2937.5	3742.9	3554.46	4742.9
135 °C	863.3	1157.78	936.56	1215.32	1150.1	1498.1
155 °C	285.04	380.48	315.82	406.06	397.24	520.18

Post-RTFO aging, the viscosity increase for NS is the most pronounced, indicating a heightened sensitivity to aging. At the 135 °C measurement, NS's average viscosity climbs

by 33% from its original state. Meanwhile, NT and NA show less significant aging effects, with increases of 25% and 21%, respectively. Despite these changes, it is recognized that post-aging viscosities are not subject to the same AASHTO M320 threshold as the original binders, and the modified asphalts are still expected to have adequate workability for practical paving applications.

4.4. Mass Loss due to Aging

Figure 8 illustrates the impact of nanomaterials on the thermal aging characteristics of asphalt binders, as determined through the Rolling Thin Film Oven (RTFO) test. The graph reveals a discernible trend where the inclusion of nanomaterials, specifically NT, exhibits a potential for reducing mass loss, which is indicative of enhanced thermal stability. Initially, the addition of NT appears to mitigate the aging process, with mass loss decreasing to 0.234% at a 2% dosage, representing a reduction of 12% from the control. Even at an 8% inclusion, the mass loss for NT is 0.259%, which is only marginally lower than the control, suggesting that NT may act as an anti-aging agent, hinting at a complex interaction between NT and the binder as concentrations increase.
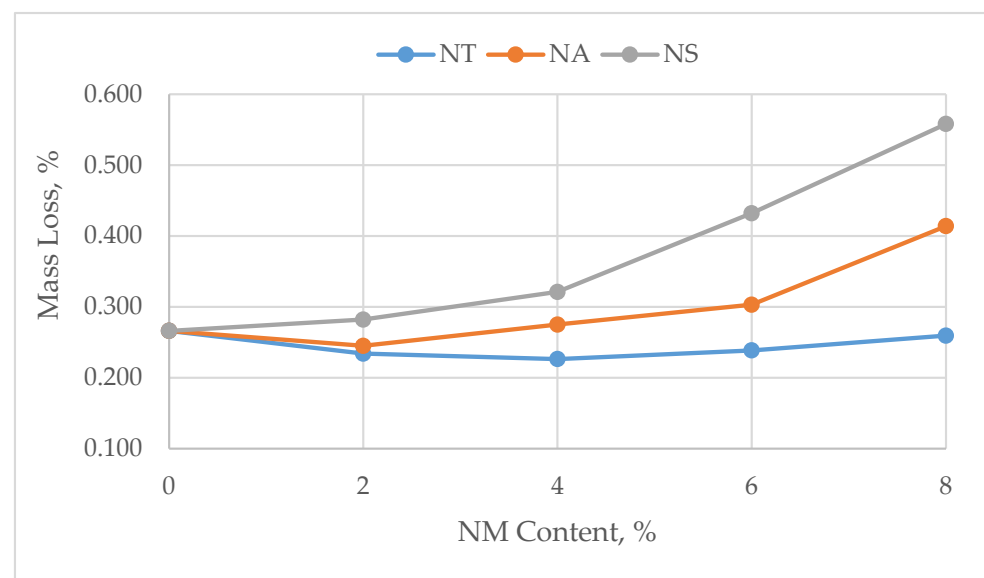

Figure 8. Effect of nanomaterials on mass loss due to RTFO.

Conversely, binders amended with NA and NS demonstrate a clear and direct increase in mass loss as the nanomaterial content escalates. NA sees a marked rise from the baseline mass loss to 0.414% at an 8% addition, translating to a significant increase of 55.64%. NS exhibits an even more pronounced uptick, with the mass loss reaching 0.558% at an 8% inclusion, representing an increase of 109.77% compared to the control. These results suggest that NA and NS, perhaps due to their specific surface interactions and higher binder affinity, contribute to a more substantial release of volatile compounds, thereby more intensely affecting the binder's thermal stability compared to NT.

When ranking the nanomaterials concerning aging resistance, NT appears to offer the best performance at low to moderate concentrations. In contrast, NA and NS, while enhancing certain binder properties, seem to decrease aging resistance. Despite the variations in mass loss with different nanomaterial contents, it is noteworthy that all modified binders remain within the acceptable limit of less than a 1% mass loss as stipulated by [41] for RTFO aged asphalt. This confirms that, within the investigated range, the nanomaterials do not compromise the asphalt's resistance to aging, thereby maintaining the prescribed standards for durability and performance.

4.5. Rheological Properties

The rheological properties of asphalt binders, as determined by the Dynamic Shear Rheometer (DSR) test, provide essential insights into the binder's resistance to deformation and fatigue life. This series of tests, presented in Figures 9–11, assess the performance in terms of the rutting factor (G*/sin δ) for the original, RTFO-aged, and PAV-aged samples, along with the fatigue factor (G* sin δ) post-PAV conditioning.
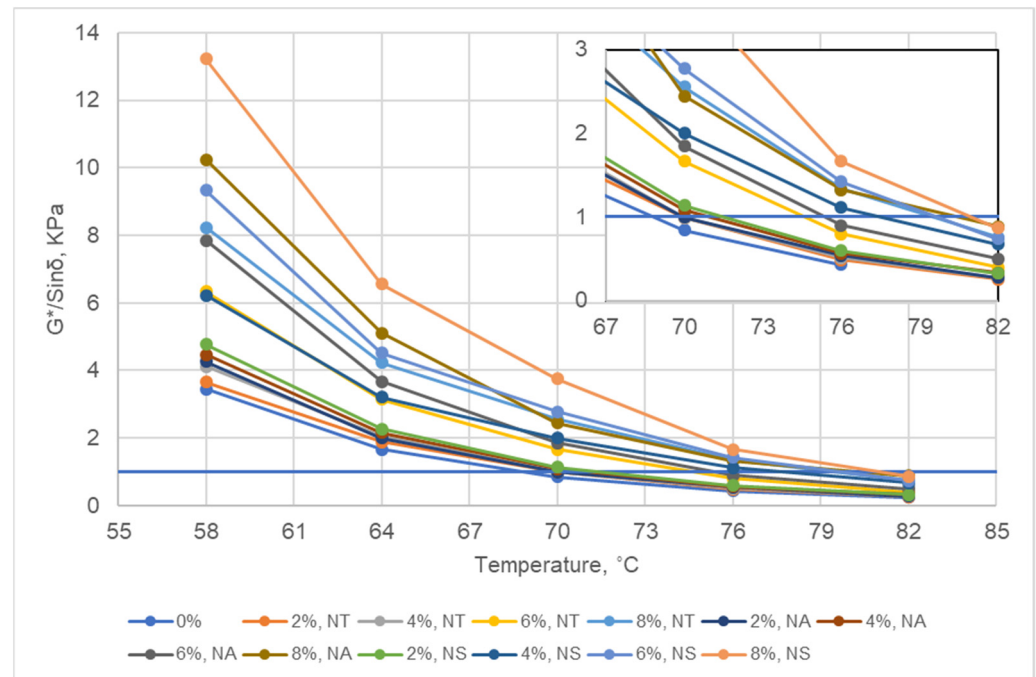

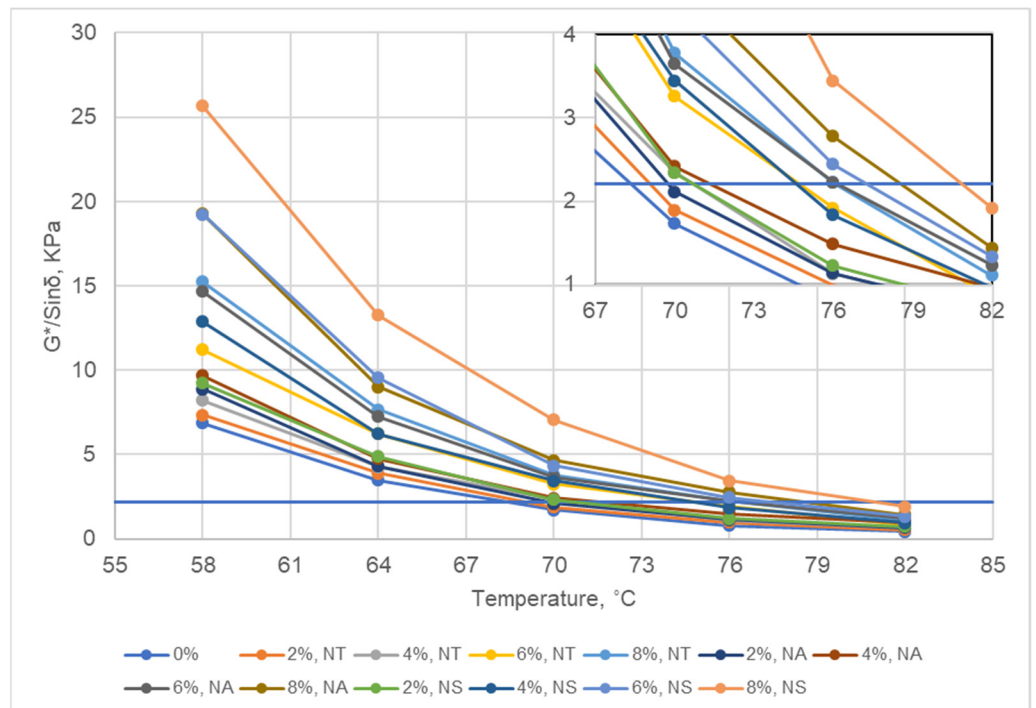**Figure 9.** Results of DSR of original binder.

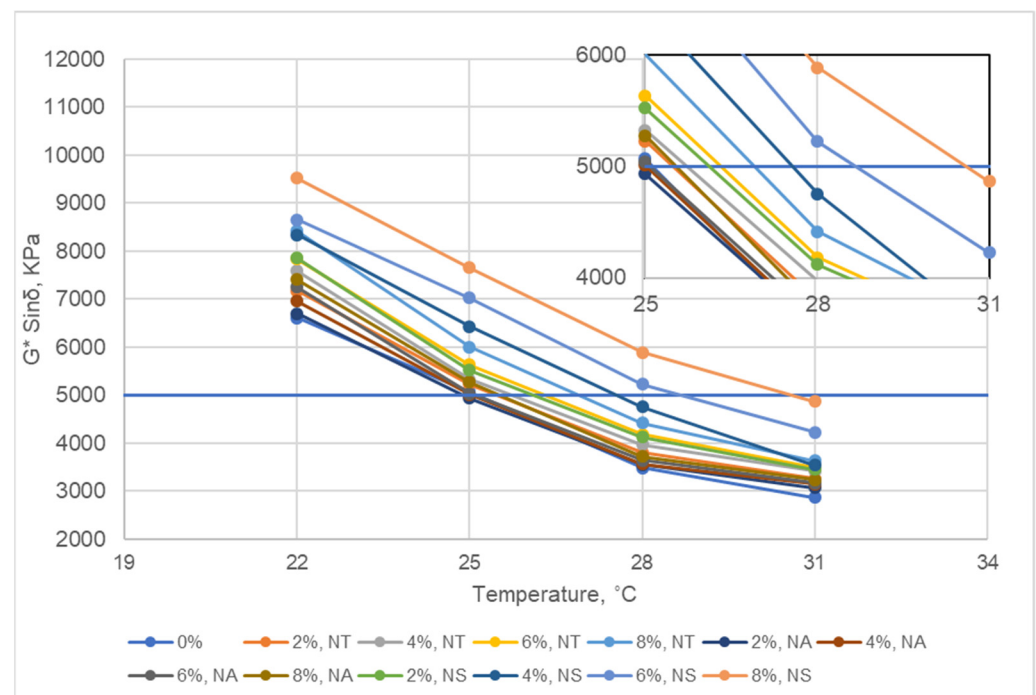**Figure 10.** Results of DSR after RTFO.

Figure 11. Results of DSR after PAV.

For the original binders, Figure 9 shows that the inclusion of nanomaterials such as NT, NA, and NS leads to an increase in the G*/sin δ values across various temperatures, signifying an improved resistance to permanent deformation. Specifically, the NT-modified binder demonstrates a significant increase in the rutting parameter, indicating an enhanced capacity to withstand rutting at elevated temperatures.

Upon RTFO aging, as depicted in Figure 10, all nanomaterial-modified binders exhibit increased rutting resistance. However, the degree of improvement varies with each nanomaterial type, with NS showing the highest rutting factor, followed by NA and NT. This trend suggests that NS is particularly effective in enhancing high-temperature performance, potentially extending the service life of pavements subjected to heavy traffic loads.

The fatigue resistance of the binders, reflected in the fatigue factor (G* sin δ) after PAV aging, is illustrated in Figure 11. Here, the data indicate a trade-off between increased stiffness and fatigue life. While nanomaterials contribute to higher stiffness, as indicated by the elevated G* sin δ values, this also implies a slight increase in the risk of fatigue cracking. Despite this, the enhancements in rutting resistance may offset the marginal reduction in fatigue life, especially in regions with high temperature variations.

When ranking the nanomaterials based on their effects on the rutting index (G*/sin δ) and fatigue index (G* sin δ), SiO_2 emerges as the most effective in improving rutting resistance, with the recommended optimal dosage being 6%. For fatigue resistance, NT at a dosage of 4% is preferable, as it presents a balanced modification, increasing the stiffness without unduly compromising the binder's fatigue life.

In conclusion, the strategic selection and concentration of nanomaterials are pivotal in modifying asphalt binders, as evidenced by the DSR results. NS stands out for its rutting resistance, while NT offers a balanced enhancement in both rutting and fatigue indices. Optimal dosages should be carefully considered to maximize performance benefits and ensure the durability and longevity of asphalt pavements.

5. Optimal Nanomaterial Content

Overall Desirability (OD) is a multi-criteria decision analysis method employed to ascertain optimal conditions that satisfy multiple objectives. This research utilizes an OD analysis to determine the most effective nanomaterial dosage for modifying asphalt binders.

The method assesses a range of investigated properties, including penetration (X1), the softening point (X2), Penetration Index (X3), mass loss due to RTFO aging (X4), storage stability (X5), viscosity at 135 °C before aging (X6), the temperature at which the rutting index (G*/sin δ) equals 1 kPa for the original binder (X7), and 2.2 kPa for the RTFO-aged binder (X8), along with the temperature corresponding to a fatigue index (G* sin δ) of 5000 kPa (X9).

The OD calculation involves normalizing each of these values on a scale from 0 to 1, where 1 represents the most desirable outcome. The normalization approach can be carried out by using either the maximum value of the properties (the larger the better) or the minimum (the smaller the better) value of the properties in terms of Equation (2) or (3), respectively. For Equation (2), the larger the normalization data, the better the OD, but for Equation (3), it is the opposite.

$$x_i^*(k) = \frac{x_i^{(0)}(k) - minx_i^{(0)}}{maxx_i^{(0)} - minx_i^{(0)}} \tag{2}$$

$$x_i^*(k) = \frac{maxx_i^{(0)} - x_i^{(0)}(k)}{maxx_i^{(0)} - minx_i^{(0)}} \tag{3}$$

where i = 1, 2,..., m (m is the index number); k = 1, 2,..., n (n is the data number); $x_i^{(0)}(k)$ is the kth value of the ith original sequence; $x_i^*(k)$ is the k-th value of the i-th normalized sequence; $maxx_i^{(0)}$ i is the maximum value of the i-th original sequence; and $minx_i^{(0)}$ is the minimum value of the i-th original sequence.

The normalized values are subsequently combined using a geometric mean to compute the OD score for each nanomaterial dosage level, aiding in the identification of the optimal dosage that maximizes the desired characteristics of the modified asphalt binder as per Equation (4).

$$\gamma(k) = [x_1^*(k)x_1^*(k)\ldots..x_m^*(k)]^{1/m} \tag{4}$$

Higher OD scores denote a more favorable combination of properties, thus proving to be essential tools for researchers and engineers to pinpoint the optimal nanomaterial content that enhances asphalt binder performance. Upon examining Tables 7–9, which present the normalized indices and Overall Desirability (OD) for NT-, NA-, and NS-modified asphalt, it is evident that both NT and NA achieve a peak OD at a 6% nanomaterial content, indicating an optimal improvement in asphalt binder properties. This dosage notably improves resistance to deformation, as evidenced by the temperature at which the rutting index equals 1 kPa, which is vital for good performance under high temperatures.

For NA-modified asphalt, the 6% inclusion level is distinguished by its enhanced rutting resistance while still offering satisfactory fatigue resistance, as denoted by the fatigue index at 5000 kPa. Although it does not provide the highest fatigue resistance, this concentration delivers a beneficial equilibrium among critical properties such as the softening point, penetration, and mass loss due to aging.

In the case of NS-modified asphalt, the OD analysis indicates that a 4% inclusion rate is the most favorable. At this concentration, properties such as penetration, the softening point, and resistance to rutting and fatigue are significantly improved without incurring excessive mass loss due to aging. This suggests that a 4% NS content yields the best balance between enhancing the binder properties and maintaining stability, making it the optimal dosage for NS-modified asphalt within the scope of this study.

In summary, the OD method effectively consolidates diverse rheological and performance measures into a single metric, enabling the identification of the most advantageous nanomaterial concentration. NT- and NA-modified asphalts display improved binder attributes at a 6% nanomaterial dosage, whereas NS-modified asphalt reaches peak performance at a 4% inclusion rate, thereby establishing these as the optimum concentrations for ameliorating asphalt binder characteristics per the parameters analyzed. These findings

highlight the importance of careful nanomaterial dosage selection to maximize the overall performance of asphalt mixes. The OD values serve as a quantitative measure, guiding the selection of the most effective nanomaterial content for the desired asphalt properties.

Table 7. The original values, normalized values, and OD for NT-modified asphalt.

Test	Parameter	NT Content, %				
		0	2	4	6	8
Penetration, 1/10 mm	$X_1^{(0)}$	49	48	45	42	40
	X_1^*	0.000	0.111	0.444	0.778	1.000
Softening point, °C	$X_2^{(0)}$	49.7	50	50.4	51.5	53.1
	X_2^*	0.000	0.088	0.206	0.529	1.000
PI	$X_3^{(0)}$	−1.33	−1.3	−1.34	−1.22	−0.96
	X_3^*	0.026	0.105	0.300	0.316	1.000
Mass loss, %	$X_4^{(0)}$	0.266	0.234	0.226	0.238	0.259
	X_4^*	0.000	0.808	1.000	0.695	0.169
Storage stability, °C	$X_5^{(0)}$	0.4	0.8	1.3	1.7	2
	X_5^*	1.000	0.750	0.438	0.188	0.000
RV at 135 °C, mPa·s	$X_6^{(0)}$	719.7	793.1	904.4	916.8	982.5
	X_6^*	0.000	0.279	0.703	0.750	1.000
Temp (°C) at rutting index = 1 kPa	$X_7^{(0)}$	68.85	69.92	69.93	74.61	79.47
	X_7^*	0.000	0.101	0.102	0.542	1.000
Temp (°C) at rutting index = 2.2 kPa	$X_8^{(0)}$	68.35	69.06	70.68	74.71	76.08
	X_8^*	0.000	0.092	0.301	0.823	1.000
Temp (°C) at fatigue index = 5000 kPa	$X_9^{(0)}$	25.13	25.48	25.72	26.31	26.89
	X_9^*	1.000	0.801	0.665	0.330	0.000
Overall Desirability (OD)		0.000	0.222	0.382	0.498	0.000

Table 8. The original values, normalized values, and OD for NA-modified asphalt.

Test	Parameter	NA Content, %				
		0	2	4	6	8
Penetration, 1/10 mm	$X_1^{(0)}$	49	47	44	41	36
	X_1^*	0.000	0.154	0.385	0.615	1.000
Softening point, °C	$X_2^{(0)}$	49.7	50.1	51.1	52.9	54.6
	X_2^*	0.000	0.082	0.286	0.653	1.000
PI	$X_3^{(0)}$	−1.33	−1.32	−1.22	−0.95	−0.85
	X_3^*	0.000	0.021	0.229	0.792	1.000
Mass loss, %	$X_4^{(0)}$	0.266	0.245	0.275	0.303	0.414
	X_4^*	0.876	1.000	0.822	0.657	0.000
Storage stability, °C	$X_5^{(0)}$	0.4	0.6	0.9	1.3	1.6
	X_5^*	1.000	0.833	0.583	0.250	0.000
RV at 135 °C, mPa·s	$X_6^{(0)}$	719.7	845.2	965.9	1063	1089
	X_6^*	1.000	0.660	0.333	0.070	0.000
Temp (°C) at rutting index = 1 kPa	$X_7^{(0)}$	68.85	69.97	70.91	75.36	80.42
	X_7^*	0.000	0.097	0.178	0.563	1.000
Temp (°C) at rutting index = 2.2 kPa	$X_8^{(0)}$	68.35	69.75	71.36	76.14	78.57
	X_8^*	0.000	0.137	0.295	0.762	1.000
Temp (°C) at fatigue index = 5000 kPa	$X_9^{(0)}$	25.13	24.88	25.02	25.08	25.53
	X_9^*	0.615	1.000	0.785	0.692	0.000
Overall Desirability (OD)		0.000	0.231	0.380	0.469	0.000

Table 9. The original values, normalized values, and OD for NS-modified asphalt.

Test	Parameter	NS Content, %				
		0	2	4	6	8
Penetration, 1/10 mm	$X_1^{(0)}$	49	47	43	37	29
	X_1^*	0.000	0.100	0.300	0.600	1.000
Softening point, °C	$X_2^{(0)}$	49.7	50.9	52.1	53.2	55.7
	X_2^*	0.000	0.200	0.400	0.583	1.000
PI	$X_3^{(0)}$	−1.33	−1.12	−1.03	−1.1	−1.04
	X_3^*	0.000	0.700	1.000	0.767	0.967
Mass loss, %	$X_4^{(0)}$	0.266	0.282	0.321	0.432	0.558
	X_4^*	1.000	0.945	0.812	0.432	0.000
Storage stability, °C	$X_5^{(0)}$	0.4	0.6	0.7	0.9	1.3
	X_5^*	1.000	0.778	0.667	0.444	0.000
RV at 135 °C, mPa·s	$X_6^{(0)}$	719.7	804.9	1129.3	1325.8	1770.8
	X_6^*	1.000	0.919	0.610	0.423	0.000
Temp (°C) at rutting index = 1 kPa	$X_7^{(0)}$	68.85	71.53	77.56	79.72	81
	X_7^*	0.000	0.221	0.717	0.895	1.000
Temp (°C) at rutting index = 2.2 kPa	$X_8^{(0)}$	68.35	70.71	74.61	77.3	80.87
	X_8^*	0.000	0.188	0.500	0.715	1.000
Temp (°C) at fatigue index = 5000 kPa	$X_9^{(0)}$	25.13	26.12	27.56	28.67	30.6
	X_9^*	1.000	0.819	0.556	0.353	0.000
Overall Desirability (OD)		0.000	0.409	0.584	0.554	0.000

6. Conclusions

Based on experimental evaluations of asphalt binders modified with Nano-Titanium Dioxide (NT), Nano-Aluminum Oxide (NA), and Nano-Silica Oxide (NS) at various dosages ranging from 0% to 8%, the following conclusions are drawn:

1. The SEM analysis highlights unique morphologies of the nanomaterials used. NT displays spherical clusters, suggesting efficient dispersion within asphalt. NA is characterized by irregular agglomerates, potentially influencing its interaction with the binder. NS reveals a dense arrangement of particles, indicative of a significant surface area, which is crucial for integrating with the asphalt binder. These morphological traits are fundamental in understanding the interaction of each nanomaterial with the asphalt matrix.
2. NS-modified asphalt demonstrated the best storage stability with a 225% increase in ΔT at an 8% inclusion compared to a 400% increase for NT and a 300% increase for NA, highlighting NS's superior homogeneity.
3. All modified binders remained within acceptable viscosity limits after RTFO aging. NS had the highest average viscosity increase of 33% compared to neat asphalt, suggesting its significant impact on the binder's viscosity.
4. TiO_2 reduced mass loss by 12% at a 2% dosage, demonstrating potential anti-aging properties. In contrast, Al_2O_3 and SiO_2 increased the mass loss by 55.64% and 109.77%, respectively, at an 8% inclusion, affecting thermal stability differently.
5. SiO_2 markedly improved the rutting resistance, showing the highest rutting factor, making it effective for high-temperature performance and heavy traffic conditions.
6. Nanomaterials increased the binder stiffness, with the G* sin δ values indicating a slightly higher risk of fatigue cracking. However, the benefits in rutting resistance may offset this risk.
7. The optimal dosage for enhanced performance was identified as 6% for both NT and NA, while NS achieved the best balance of properties at a 4% inclusion rate. This suggests that a nuanced approach is required when selecting nanomaterial dosages to maximize the overall asphalt binder's performance.

8. Further field testing and evaluations are recommended to ensure enhanced pavement performance and to confirm the technical viability and practical applicability of NT, NA, and NS in practical pavement applications.

In summary, this study provides comprehensive insights into the effects of nanomaterial additives, namely NT, NA, and NS, on asphalt binder performance by systematically analyzing dosages ranging from 0% to 8%. This study establishes that NS significantly enhances rutting resistance, making it suitable for high-temperature and heavy-load applications. Despite the increase in binder stiffness leading to a potential rise in fatigue risk, the overall improvements in performance characteristics suggest that nanomaterial additives can substantially benefit pavement quality and longevity. The identified optimal dosages of 6% for NT and NA and 4% for NS provide a guideline for utilizing these nanomaterials to bridge the gap between traditional materials and modern pavement requirements. Further field testing is recommended to validate these findings and ensure their practical applicability in real-world scenarios.

References

1. Al-bayati, A.H.K.; Lateif, R.H. Evaluating the performance of high modulus asphalt concrete mixture for base course in Iraq. *J. Eng.* **2017**, *23*, 14–33. [CrossRef]
2. Mirzamojeni, M.; Aghayan, I.; Behzadian, R. Evaluation of field aging effect on self-healing capability of asphalt mixtures. *Constr. Build. Mater.* **2023**, *369*, 130571. [CrossRef]
3. Fusco, R.; Moretti, L.; Fiore, N.; D'Andrea, A. Behavior evaluation of bituminous mixtures reinforced with nano-sized additives: A review. *Sustainability* **2020**, *12*, 8044. [CrossRef]
4. Al-Taher, M.; Hassanin, H.; Ibrahim, M.F.; Sawan, A.M. Comparative study of performance of modified asphalt mixtures using different traditional and nano additives. *Int. J. Sci. Eng. Res.* **2018**, *9*, 3.
5. Korniejenko, K.; Nykiel, M.; Choinska, M.; Jexembayeva, A.; Konkanov, M.; Aruova, L. An Overview of Micro-and Nano-Dispersion Additives for Asphalt and Bitumen for Road Construction. *Buildings* **2023**, *13*, 2948. [CrossRef]
6. Mohammed, A.M.; Abed, A.H. Enhancing asphalt binder performance through nano-SiO_2 and nano-$CaCO_3$ additives: Rheological and physical insights. *Case Stud. Constr. Mater.* **2023**, *19*, e02492. [CrossRef]
7. Li, R.; Xiao, F.; Amirkhanian, S.; You, Z.; Huang, J. Developments of nano materials and technologies on asphalt materials-A review. *Constr. Build. Mater.* **2017**, *143*, 633–648. [CrossRef]
8. Ali, M.; Albayati, A.H.K.; Wang, Y. A review of interface bonding testing techniques. *J. Coeng.* **2023**, *29*, 14–30. [CrossRef]
9. Farina, A.; Kutay, M.E.; Anctil, A. Environmental assessment of asphalt mixtures modified with polymer coated rubber from scrap tires. *J. Clean. Prod.* **2023**, *418*, 138090. [CrossRef]
10. Al-Azawee, E.T.; Latief, R.H. The feasibility of using styrene-butadiene-styrene (SBS) as modifier in Iraqi bituminous binder. *J. Eng. Sci. Technol.* **2020**, *15*, 1596–1607.
11. Rondón-Quintana, H.A.; Ruge-Cárdenas, J.C.; Zafra-Mejía, C.A. Natural asphalts in pavements: Review. *Sustainability* **2023**, *15*, 2098. [CrossRef]
12. Mohammed, F.A.; Latief, R.H.; Albayati, A.H.K. Assessment of traditional asphalt mixture performance using natural asphalt from sulfur springs. *J. Coeng.* **2024**, *30*, 54–73. [CrossRef]

13. Wang, Y.; Latief, R.H.; Al-Mosawe, H.; Mohammad, H.K.; Albayati, A.; Haynes, J. Influence of iron filing waste on the performance of warm mix asphalt. *Sustainability* **2021**, *13*, 13828. [CrossRef]

14. Li, J.; Tang, F. Effects of two metal nanoparticles on performance properties of asphalt binder and stone matrix asphalt mixtures containing waste high density polyethylene. *Constr. Build. Mater.* **2023**, *401*, 132787. [CrossRef]

15. Hashim, S.; Al-Mosawe, H.; Mohammed, H. The Influence of Using Recycled Asphalt Pavement and Crumbed Rubber on Asphalt Pavement: A Review. *Al-Nahrain J. Eng. Sci.* **2023**, *26*, 74–82. [CrossRef]

16. Lima, O.; Afonso, C.; Segundo, I.R.; Landi, S.; Homem, N.C.; Freitas, E.; Alcantara, A.; Branco, V.C.; Soares, S.; Soares, J.; et al. Asphalt binder "Skincare"? Aging evaluation of an asphalt binder modified by nano-TiO$_2$. *Nanomaterials* **2022**, *12*, 1678. [CrossRef]

17. Aljbouri, R.Q.; Albayati, A.H.K. Investigating the effect of nanomaterials on the marshall properties and durability of warm mix asphalt. *Cogent Eng.* **2023**, *10*, 2269640. [CrossRef]

18. Diab, A.; You, Z.; Hossain, Z.; Zaman, M. Moisture susceptibility evaluation of nanosize hydrated lime-modified asphalt-aggregate systems based on surface free energy concept. *Transp. Res. Rec.* **2024**, *2446*, 52–59. [CrossRef]

19. Yusoff, N.I.M.; Breem, A.A.S.; Alattug, H.N.M.; Ahmad, A.H.J. The effects of moisture susceptibility and ageing conditions on nano-silica/polymer-modified asphalt mixtures. *Constr. Build. Mater.* **2014**, *72*, 139–147. [CrossRef]

20. Martínez-Toledo, C.; Valdés-Vidal, G.; Calabi-Floody, A.; González, M.E.; Reyes-Ortiz, O. Effect of biochar from oat hulls on the physical properties of asphalt binder. *Materials* **2022**, *15*, 7000. [CrossRef]

21. Ghabchi, R. Effect of Lignin Type as an Additive on Rheology and Adhesion Properties of Asphalt Binder. *Solids* **2022**, *3*, 603–619. [CrossRef]

22. Ji, H.; He, D.; Li, B.; Lu, G.; Wang, C. Evaluation of rheological and anti-aging properties of TPU/nano-TiO2 composite-modified asphalt binder. *Materials* **2022**, *15*, 3000. [CrossRef] [PubMed]

23. Yang, S.; Yan, K.; Liu, W. The effect of ultraviolet aging duration on the rheological properties of sasobit/SBS/Nano-TiO2-Modified asphalt binder. *Appl. Sci.* **2022**, *12*, 10600. [CrossRef]

24. Hassan, M.M.; Mohammad, L.N.; Cooper, S.B.; Dylla, H. Evaluation of nano-titanium dioxide additive on asphalt binder aging properties. *Transp. Res. Rec.* **2011**, *2207*, 11–15. [CrossRef]

25. Zhang, H.; Zhu, C.; Yu, J.; Shi, C.; Zhang, D. Influence of surface modification on physical and ultraviolet aging resistance of bitumen containing inorganic nanoparticles. *Constr. Build. Mater.* **2015**, *98*, 735–740. [CrossRef]

26. Mubaraki, M.; Ali, S.I.A.; Ismail, A.; Yusoff, N.I.M. Rheological evaluation of asphalt cements modified with ASA polymer and Al$_2$O$_3$ nanoparticles. *Procedia Eng.* **2016**, *143*, 1276–1284. [CrossRef]

27. Saltan, M.; Terzi, S.; Karahancer, S. Examination of hot mix asphalt and binder performance modified with nano silica. *Constr. Build. Mater.* **2017**, *156*, 976–984. [CrossRef]

28. Chelovian, A.; Shafabakhsh, G. Laboratory evaluation of nano Al$_2$O$_3$ effect on dynamic performance of stone mastic asphalt. *Int. J. Pavement Res. Technol.* **2017**, *10*, 131–138. [CrossRef]

29. Enieb, M.; Diab, A. Characteristics of asphalt binder and mixture containing nanosilica. *Int. J. Pavement Res. Technol.* **2017**, *10*, 148–157. [CrossRef]

30. Shi, X.; Cai, L.; Xu, W.; Fan, J.; Wang, X. Effects of nano-silica and rock asphalt on rheological properties of modified bitumen. *Constr. Build. Mater.* **2018**, *161*, 704–714. [CrossRef]

31. Qian, G.; Yu, H.; Gong, X.; Zhao, L. Impact of nano-TiO$_2$ on the NO$_2$ degradation and rheological performance of asphalt pavement. *Constr. Build. Mater.* **2019**, *218*, 53–63. [CrossRef]

32. Buhari, R.; Abdullah, M.E.; Ahmad, M.K.; Zabidi, N.; Abu Bakar, S.K. Moisture susceptibility of modified asphalt concrete containing titanium dioxide. *Int. J. Adv. Trends Comp. Sci. Eng.* **2019**, *8*, 140–143. [CrossRef]

33. Taherkhani, H.; Tajdini, M. Comparing the effects of nano-silica and hydrated lime on the properties of asphalt concrete. *Constr. Build. Mater.* **2019**, *218*, 308–315. [CrossRef]

34. Günay, T.; Ahmedzade, P. Physical and rheological properties of nano-TiO$_2$ and nanocomposite modified bitumens. *Constr. Build. Mater.* **2020**, *243*, 118208. [CrossRef]

35. Karahancer, S. Effect of aluminum oxide nano particle on modified bitumen and hot mix asphalt. *Pet. Sci. Technol.* **2020**, *38*, 773–784. [CrossRef]

36. Bhat, F.S.; Mir, M.S. Investigating the effects of nano Al$_2$O$_3$ on high and intermediate temperature performance properties of asphalt binder. *Road Mater. Pavement Des.* **2021**, *22*, 2604–2625. [CrossRef]

37. Bhat, F.S.; Mir, M.S. A study investigating the influence of nano Al$_2$O$_3$ on the performance of SBS modified asphalt binder. *Constr. Build. Mater.* **2021**, *271*, 121499. [CrossRef]

38. Masri, K.A.; Zali, N.S.S.M.; Jaya, R.P.; Seman, M.A.; Rosli, M.R.M. The influence of nano titanium as bitumen modifier in stone mastic asphalt. *Adv. Mater. Sci. Eng.* **2022**, *2022*, 4021618. [CrossRef]

39. Alas, M.; Abba, S.I.; Ali, S.I.A.; Rahim, A.; Yusoff, N.I.M. Evaluating the performance of aluminum oxide nanoparticle-modified asphalt binder and modelling the viscoelastic properties by using artificial neural networks and support vector machines. *Adv. Mater. Sci. Eng.* **2022**, *2022*, 9685454. [CrossRef]

40. Taher, Z.K.; Ismael, M.Q. Moisture susceptibility of hot mix asphalt mixtures modified by nano silica and subjected to aging process. *J. Coeng.* **2023**, *29*, 128–143. [CrossRef]

41. *AASHTO M 320*; Standard Specification for Performance-Graded Asphalt Binder. American Association of State Highway and Transportation Officials: Washington, DC, USA, 2013.
42. *AASHTO T 49*; Standard Test Method for Penetration of Bituminous Materials. American Association of State Highway and Transportation Officials: Washington, DC, USA, 2020.
43. *AASHTO T 51*; Standard Test Method for Ductility of Asphalt Materials. American Association of State Highway and Transportation Officials: Washington, DC, USA, 2020.
44. *AASHTO T 48*; Standard Test Method for Flash and Fire Points by Cleveland Open Cup. American Association of State Highway and Transportation Officials: Washington, DC, USA, 2020.
45. *AASHTO T 53*; Standard Test Method for Softening Point of Bitumen (Ring-and-Ball Apparatus). American Association of State Highway and Transportation Officials: Washington, DC, USA, 2020.
46. *ASTM D7173-20*; Standard Practice for Determining the Separation Tendency of Polymer from Polymer Modified Asphalt. ASTM: West Conshohocken, PA, USA, 2020.
47. *ASTM D2872-22*; Standard Test Method for Effect of Heat and Air on a Moving Film of Asphalt (Rolling Thin-Film Oven Test). ASTM: West Conshohocken, PA, USA, 2020.
48. *ASHTO TP48*; Standard Test Method for Viscosity Determination of Asphalt Binder Using Rotational Viscometer. American Association of State Highway and Transportation Officials: Washington, DC, USA, 2020.
49. *AASHTO T315*; Standard Method of Test for Determining the Rheological Properties of Asphalt Binder Using a Dynamic Shear Rheometer (DSR). American Association of State Highway and Transportation Officials: Washington, DC, USA, 2020.